Hindawi
Advances in Civil Engineering
Volume 2022, Article ID 8578684, 10 pages
https://doi.org/10.1155/2022/8578684

Research Article

Experimental Study on Stability of Long-Span PC Cable-Stayed Bridge during the Construction Periods

Yong Zeng,[1] **Yuxiao Wang**,[2] **Zhenwei Shi**,[1] **Hongmei Tan**,[2] **and Anbang Gu**[2]

[1]*State Key Laboratory of Mountain Bridge and Tunnel Engineering, Chongqing Jiaotong University, Chongqing, China*
[2]*Mountain Bridge and Materials Engineering Research Center of Ministry of Education, Chongqing Jiaotong University, Chongqing, China*

Correspondence should be addressed to Yong Zeng; yongzeng@cqjtu.edu.cn

Received 14 January 2022; Accepted 14 June 2022; Published 9 August 2022

Academic Editor: Luigi Fenu

With the increasing span of cable-stayed bridges, the towers are getting higher and higher, and the stiffening beams are becoming more and more slender. The increase in span causes the axial pressure of the beams and towers to increase rapidly, and the sag effect of the cables, geometric nonlinearity, and material nonlinear effects are significantly increased. The influence of these disadvantages greatly reduces the stability of the cable-stayed bridge, and the stability of the cable-stayed bridge becomes prominent. In this paper, the finite element method is used to analyze the first kind of stability problem and the second kind of stability problem of cable-stayed bridges. On this basis, a large-span prestressed concrete (PC) cable-stayed bridge is taken as an example to analyze and compare the two types of stability problems of the bridge during the construction phase and the operation phase. Besides, the model experimental study on the stability of the bridge during the maximum double cantilever construction period was carried out. The theoretical values and the model test results are compared to verify the correctness of the calculation method and design theory, which may provide a reference for the design, construction, and scientific research of cable-stayed bridges.

1. Introduction

Stromsund Bridge, built in Sweden in 1956, is generally regarded as the beginning of a modern cable-stayed bridge with a span of 75 + 183 + 75 m and a composite beam of reinforced concrete slab and steel plate girder. In the early 1960s, structural analysis made a new breakthrough [1]. The use of electronic computers to analyze the statically indeterminate structure led to the emergence of multicable systems and laid the foundation for the widespread promotion of cable-stayed bridges [2]. Over the past 60 years, nearly 1000 cable-stayed bridges are built around the world.

The cable-stayed bridge is a composite structure consisting of cable towers, cables, and main beams. The cable tower and the main beam are pressure-bearing members mainly subjected to pressure, while the cable is only subjected to tensile force. The main beam of the cable-stayed bridge works under the support of the stayed cables, just like the multispan elastic support continuous beam, which can greatly reduce the bending moment of the main beam and improve the forced state of the main beam. Moreover, the height of the main beam is small and does not increase with the increase of the bridge span, so it can cross a large space. The horizontal component force of the cable force is transferred as the axial force of the main beam. For the prestressed concrete (PC) main beam with high compressive resistance capacity and low tensile capacity, not only can the mechanical properties of the high-strength material be fully utilized but also the strength and crack resistance of the main beam can be increased [3].

Stability problem is one of the key problems that need to be solved in the design and construction of bridge structures under pressure [4]. The research on the stability of structures such as arch bridges, which are obviously dominated by compression, has a long history. The research work is comprehensive and in-depth, and the research results

basically meet the development needs of arch bridges. However, the stability of cable-stayed bridges has not received much attention in the early stages of development, and there are fewer studies on this. With the increasing span of cable-stayed bridges, increase in structural types, and change in structural systems (such as single towers or multiple towers, single-cable-plane or multicable-plane cable-stayed bridges, and cable-stayed suspension bridges), a deeper understanding of the structural behavior of cable-stayed bridges were got, more attention on the stability of cable-stayed bridges was also received, and some studies were carried out, but these studies are mainly carried out for parts such as the tower and the stiffening beam. The main tower, main beam, and stay cable of the cable-stayed bridge are connected as a whole, coupled, and affected each other. The calculation method of its stability should not be calculated separately for the bridge tower or main beam, but for the whole. With the increase of the span of cable-stayed bridge, the slenderness ratio of the tower and stiffening girder, the material performance and working performance of the bridge constantly change, and the stability of the cable-stayed bridge will be affected by more factors, including material and geometric nonlinearity [5]. Cheng et al. [6] proposed that the large span cable-stayed bridge had large spatial deformation under vertical and lateral loads, and its stability problem had strong nonlinear and three-dimensional effects, which cannot be solved by conventional linear theory. It is necessary to establish new and more detailed theories and methods that reflect the characteristics of structural deformation. Therefore, to meet the development needs of cable-stayed bridges, it is necessary to further deepen the existing research. At the same time, the overall stability and stability of the construction phase for the characteristics of long-span cable-stayed bridges will become the focus of future research [7].

As the span of the cable-stayed bridge increases, the ability of the structure to resist static instability is continuously reduced and the safety factor is greatly reduced. Therefore, the stability problem is particularly prominent. The first kind of planar stability problem is caused by vertical live loads. It is caused by the axial pressure of dead load and the bending moment of live load in beams and towers. The earlier analysis methods include Leonhard's elastic foundation beam theory and Tang's energy method. The analysis accuracy depends on the degree of approximation between the assumed buckling state and the actual buckling state, and that is an approximate numerical analysis method. For the tower, it is treated as a separate column to calculate its stability. Long-span cable-stayed bridges produce a large amount of axial pressure under the combined action of dead weight, vehicle, and wind load [8]. Once the principal stress exceeds the yield strength of the material, the material goes into the plastic state. With the increase of loads, the plastic zones are enlarged and the tangential stiffness of the structure is reduced obviously, which will eventually lead to extreme instability of the structure or main components and lead to the destruction of the bridge structure. Accurate analysis must be performed using the elastic-plastic finite displacement theory.

In the initial stage of a cable-stayed bridge, the span is small, and the analysis method of the first kind of stability problem is mainly adopted. As the span of the cable-stayed bridge increases, the influence of geometric nonlinearity and material nonlinearity increases [9], and the second kind of stability problem has become prominent. But the experimental study on the stability of long-span PC cable-stayed bridges during the construction period is less. With the increase of the span of the cable-stayed bridge, the slenderness ratio of the cable tower and the stiffening girder is getting larger, the material performance and working performance of the bridge are constantly changing, and the stability of the cable-stayed bridge will be affected by more factors. The stability of the cable-stayed bridge is discussed in the paper.

2. Stability of Cable-Stayed Bridges

Structural instability means that the equilibrium state of the structure begins to lose stability under the action of external forces. If the structure is slightly disturbed, it will appear larger displacement and deformation, or even damage [10]. At this time, although the internal force of the section does not exceed its maximum resistance, the equilibrium state of the structure has changed, and the balance of internal and external forces is impossible to be obtained with the development of deformation, so the structure may have a large displacement when the external load is basically unchanged and ultimately leads to structural damage. Deformation is a paramount index of bridge health monitoring [13].

In the elastic-plastic buckling analysis of cable-stayed bridges, the influence of material nonlinearity should be considered. When the load exceeds a certain limit, with the increase of the load, the structure will enter the elastic-plastic state from the completely elastic state, then plastic deformation will occur, and then it will enter the completely plastic state and it will get damaged. For the structures constructed with ductile materials, such as prestressed concrete, which allow plastic deformation to develop sufficiently, it is often not economical to design according to the results of elastic analysis, especially for cable-stayed bridges with statically indeterminate structures, because the elastic design does not take into account the potential further bearing capacity of the structure after the material exceeds the yield limit. In addition, the theoretical calculations show that the calculated ultimate load of instability of the cable-stayed bridge is usually larger than the yield limit of the bridge material when the material nonlinearity is not considered. Therefore, to determine the critical value of the structure at the time of unstable failure (also known as the ultimate load value), it is necessary to consider the plastic deformation of the material and perform a plastic analysis of the structure.

For cable-stayed bridges, it is necessary to consider factors such as initial eccentricity, residual stress, geometric nonlinearity, and material nonlinearity. In addition, the analysis of the elastoplastic postbuckling state can also be performed. Due to the computational complexity, the overall

and partial elastoplastic buckling of the cable-stayed bridge can be analyzed using finite element software.

The overall nonlinear instability safety factor of the cable-stayed bridge in the construction process and the completed bridge state is now defined as the ratio of the amount of load that a structure can withstand before it loses its load-carrying capacity to the design load, which is calculated using the following formula:

$$\{P_{cr}\} = \lambda\{P_{sj}\}. \quad (1)$$

In the formula, λ is the safety factor of stable bearing capacity, $\{P_{cr}\}$ is the total load (including dead load and live load) of the structure under certain conditions, and $\{P_{sj}\}$ is the design load of the structure under certain conditions (including dead load and live load).

The key to structural analysis with finite elements is to simplify the structure model in accordance with the actual situation. According to the complexity of the structure and the design requirements, different calculation models are adopted, including flat or spatial, whole, or partial models. The main tower is typically modeled with a rob (beam) element. If the mechanical properties of the main beam (rigid section, vertical support) are close to the beam, the main beam can be simulated by the rob (beam) element; if the mechanical properties of the main beam are different from the beam (lateral support, large deformation of the section), then plate elements are used. In the static calculation of the cable-stayed bridge, a plane frame model or a space frame model can be used. In the buckling analysis and dynamic analysis of cable-stayed bridges, spatial calculation models are usually used.

3. FEM Calculation Model

3.1. Bridge Overview. The cable-stayed bridge studied in the paper (simplified by experimental bridge) is a PC cable-stayed bridge with two towers and two cable planes, as shown in Figure 1. Its main span is arranged: 198m + 450 m + 198 m. The total width of the bridge is 30.6 m. The main beam adopts the reinforced concrete beam and slab structure, and the beam rib height is 2.7 m. The stay cables are arranged in a fan shape. Each tower has 27 pairs of stayed cables on each side, and 110 pairs of stay cables are provided on the whole bridge. The main tower is in the shape of a vase, and the heights of the main towers in the south and the north are, respectively, 200.38 m and 206.68 m with the hollow column sections. The foundations of the north and south tower piers are group pile foundations consisting of 15 reinforced concrete piles with a diameter of 3 m.

Cable-stayed bridges are usually composed of main piers (towers), side piers, stayed cables, and main beams [13], and their structural behaviors are obviously spatial. At present, its stability analysis mainly uses spatial finite element buckling analysis. The key to finite element buckling analysis is to make a realistic model simplification of the structure [14].

When establishing the finite element model, the side piers are not simulated, but only considered its supporting

Figure 1: In situ photo of cable-stayed bridge studied in the paper.

(restraining) effect on the main beams. The main pier (tower) is a reinforced concrete hollow structure with the steel skeleton. In the finite element model, the steel skeleton is simulated with a rod element. The deck is simulated by plate elements in the horizontal plane, and the beam ribs and diaphragms are simulated by plate elements perpendicular to the horizontal plane. For prestressed tendons, rod element simulations are used in the model. In the finite element model, the rod element is used to simulate the stayed cable. The structure and load are symmetrical, but in order not to omit the buckling mode in the stability calculation, the full-bridge model is still used for calculation. The total finite element model has 13288 nodes and 33582 elements.

Because the two main pier towers (4#, 5#) of the bridge are embedded in the foundation, the root of the main pier tower is considered to be consolidated. When the bridge is completed, the main beam is a floating system. In addition to connecting the main beam with the stay cable through the main pier tower, its transverse displacement (Y direction) is constrained at the junction of the main pier tower, and its vertical and transverse displacement (Y direction and Z direction) is also constrained at the junction with the side pier. Furthermore, the caging device between the main beam and the pier is considered the elastic support constraint of the direction across the bridge. For the construction process (before the side span is closed), the main beam is temporarily fixed at the pier. Therefore, the consolidation between the main beam and the pier is considered.

The loads considered in the stability study include the first-period dead load (dead weight), the second-period dead load (bridge deck pavement, etc.), steel prestressed tendons, cable tension forces, lateral wind load, construction hanging basket, and vehicle load [15]. For the stability analysis of long-span bridges, the actual vehicle load can be converted into a uniform load along the deck. The analysis selected 13 construction states for nonlinear buckling analysis. The FEM model of the cable-stayed bridge is shown in Figure 2.

3.2. Calculation Results. The linear stability safety factor of the bridge during the construction process and the completed bridge state is generally large [16]. The stability analysis results considering nonlinearity are very different from the linear results. For the cable-stayed bridge, the overall safety factor after considering the nonlinear influence is only 1/3.3~1/5 of those of the linear analysis. In the linear stability analysis, only elastic modulus E is used to simulate the material properties, and the yield stress and failure stress

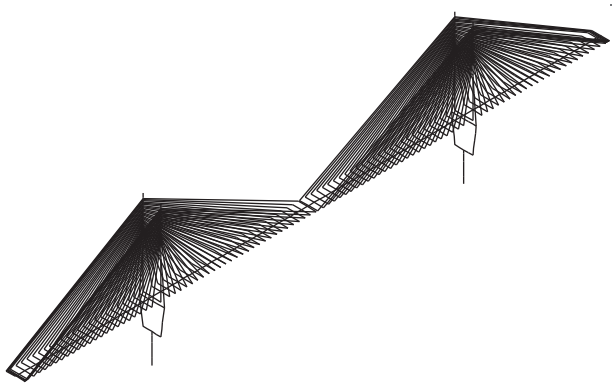

Figure 2: FEM model of a cable-stayed bridge.

of the material are not distinguished. Therefore, the calculated critical load is generally higher, but under the calculated critical load action, the stress of the structure is far higher than the failure strength limit of the material. In addition, in the linear analysis, the pull-only characteristic of the stayed cables is difficult to describe, the support effect of the simulated cable on the bridge deck in the analysis is artificially enhanced, so that the stability analysis result is high. It can be seen that for a cable-stayed bridge with large span and obvious nonlinear characteristics, the linear global buckling critical force should not be used as the final criterion for judging whether the bridge stability meets the requirements and must be considered in combination with nonlinear analysis.

In the nonlinear stability analysis, both the geometric nonlinear effect and material nonlinear effect of the structure are considered. As the load increases, the displacement of the structure increases, as shown in Figure 3. Analysis of the load-displacement curve relationship of the structure shows that the relationship between load and displacement is generally divided into three sections: the first section is a linear ascending section; the second section is a nonlinear ascending section; the third section is that when the load reaches a certain extreme value, the load begins to decrease, the displacement continues to increase, and the curve enters the falling section, which indicates that the structure has been destroyed and the bearing capacity is lost. The stability analysis after considering the nonlinear influence can truly describe the actual force characteristics of the structure, and the analysis results can truly reflect the ultimate bearing capacity of the structure.

3.3. Overall Safety Factors of the Bridge. During the formation of the main beam of the bridge, the overall stability factor of the structure gradually decreases with the advancement of the construction, but it is bigger than 4 until the bridge is completed, as shown in Figure 4. The current specification does not clearly define the overall stability factor of the cable-stayed bridge. Referring to its requirements for towers and beams, the overall structural stability factor meets the requirements (the code requirements should be greater than 4). After the completion of the bridge, the overall stability factor of the structure is the minimum,

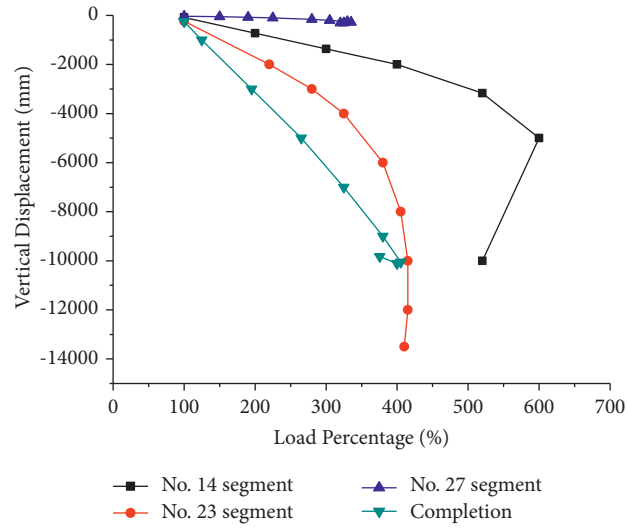

Figure 3: Vertical displacement vs. load percentage for different key construction stages.

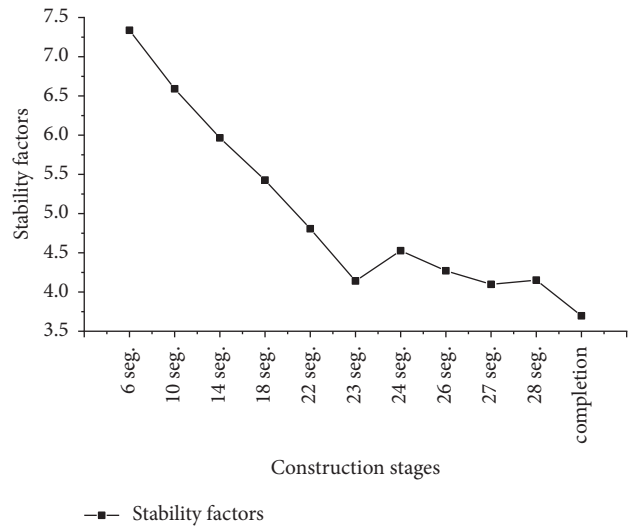

Figure 4: Analysis results of linear stability under different conditions.

3.697, under the condition of deck pavement and vehicle load. According to customary terms, it did not reach 4.0 of the specification. However, because the nonlinear instability is marked by the loss of bearing capacity, it is reasonable to use the bearing capacity safety factor to evaluate the overall stability and safety of the structure. The safety factor of the bearing capacity of the bridge reaches 3.697, which has sufficient safety.

It can be seen from the analysis in Figure 4 that the high-stress zones of the bridge tower are mainly located at the middle and lower tower columns and the lower end of the upper tower columns. The high-stress zone of the main girder is mainly located in the range of No. 1~12 segments. The magnitude of the high-stress zone and the transverse position of the main girder are different under different construction conditions. Generally speaking, the nonlinear

stable stress is more than 2.5 times the nonlinear static force. Under the conditions of No. 23 and No.27 segments completed with a small bearing capacity safety factor, the maximum stress of the main beam (located in No. 3~10 segments) is higher than the maximum stress of the tower column; when the bridge is completed and full of automobiles, the maximum stress of the tower column (mainly located in the middle tower column) is higher than the maximum stress of the main beam. This shows that, in the construction phase, the most likely form of instability failure of the structure will be the crushing of the main beam, and the most likely form of instability failure in the finished bridge state is the collapse of the tower. Given the inconvenience of stable control during the construction of the bridge, indirect control of the stress and deformation (deflection) of the structure during construction is required. It is recommended that during construction, according to the above results of nonlinear stability analysis, tracking and monitoring the segmental stresses that may occur in high-stress areas are necessary. Once the measured stress exceeds the stress obtained by nonlinear static analysis, the construction should be paused and the cause should be found as soon as possible. Thus, sudden failure of the structure can be avoided.

4. Model Experimental and Analysis

4.1. Model Design and Production. In general, the size of the model is large, and it is easy to obtain higher precision, but the model cost is high. Considering the difficulty of making the actual structure of the bridge and the requirement of measuring accuracy, the static stability experimental model has a scale ratio of 1:60; the main beam, the tower, and the main pier are made of plexiglass material; and the cable is made of high-strength steel wire rope. According to the calculation and analysis, the instability mode of the bridge in the finished bridge state is symmetrical. Considering the objective restrictive factors, only half-bridge experimental model is established.

For the convenience of production and the process of simulating the construction, the stiffening beam in the model is processed in seven segments and then bonded in the laboratory. The main beam is π-shaped rid section, seen in Figure 5. The section dimensions are similar to those of the original bridge, except that where the ribs are connected to the deck, a slight simplification is made for ease of manufacture. The height of the plexiglass tower and pier is 108.8 cm (anchorage zone of upper tower column) + 101.9 cm (middle tower column) + 63.8 cm (lower tower column) + 70 cm (main pier) = 344.5 cm. To ensure the lateral stability of the column, the middle cross beam and the lower beam are also made of plexiglass. The towers and piers are hollow boxes, and their inner and outer contour sizes are similar to the prototype, as shown in Figure 6. To anchor the pier to the ground, a 2 cm thick plexiglass plate is bonded to the root of the pier and the plate is anchored to the ground.

According to a similar relationship, the cable diameter of the model is less than 1 mm. Considering the existing commercial profiles and the safety, the full-bridge cable adopts two types of wire ropes with diameters of 2 mm and 3 mm. Among them, 0# and 24#~27# are 3 mm diameter wire ropes, and the other cables are 2 mm diameter wire ropes.

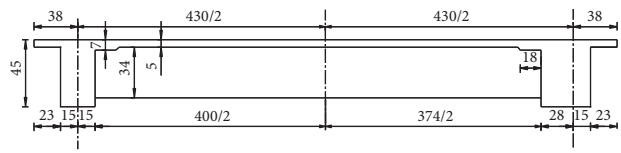

Figure 5: Cross-sectional view of the main beam of the model/mm.

The whole bridge has a total of 110 stayed cables, including 2 vertical slings. Each cable is anchored on both side walls of the main tower of the hollow box. The anchoring point of the cable on the main beam is 13.5 cm, and the cable is anchored by a special cable buckle. The cable tension adjustment is only carried out at the anchoring of the main beam. Due to the restraining effect of the side piers on the main beam, the side piers are welded with four No. 8 channel steels and the pull rods are used between the side piers. The side span anchor boxes are used to bear the bidirectional force of the bearing including tension and pressure. The actual bulk density of the plexiglass used in the model is $12kN/m^3$, so the weight of the main beam should be 504 kg. The compensation weight of the tower is 510 kg by calculation. As for the stayed cables, the weight problem is not considered.

From the data of the real bridge, it can be seen that, in the range of 2×12 m (two roadway widths), the vehicle load is$1428N/m^2$, and a similar relationship shows that the model is in the range of 2×20 cm the distributed load of the vehicle is 12.24 kg/m^2. The experimental bridge during the hoisting process is shown in Figure 7.

4.2. Calculation and Analysis of the Model. Through theoretical analysis, it is helpful to know the mechanical performance of the bridge under static load and is benefit to choose the best control section in the experiment process [17]. In addition, the instability safety factor of the text bridge and its buckling mode can be predicted, and the degree of coincidence between the calculated value and the experimental value can also be checked. Therefore, it is necessary to perform a theoretical calculation analysis on the model bridge before the model test.

In fact, when the prototype bridge is nonlinearly unstable, it is assumed that its maximum stress is $35MPa$. The stress of the model bridge is obtained by the similarity relationship, which is 3 MPa. The strain is $1000\mu\varepsilon$. According to the pure bend and tensile tests of the plexiglass material, when the bending compressive strain reaches $-5000\mu\varepsilon$ and the tensile strain reaches $3890\mu\varepsilon$, the material still is in the linear elasticity range. Moreover, the stress-strain relationship curves of the materials used for the model (plexiglass) and the materials used for the actual bridge (concrete) are also different. Therefore, simulating the nonlinear influence of plexiglass material has no great application value for the

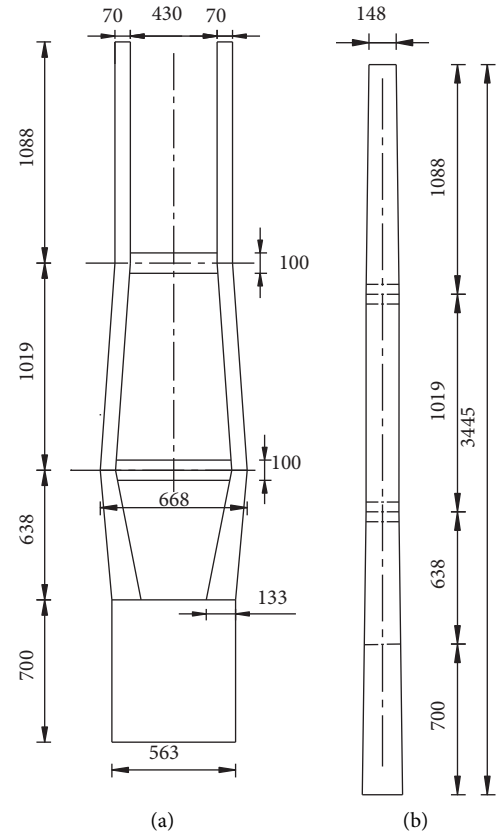

Figure 6: Across and axial direction view of the tower/mm: (a) bridge in across direction and (b) bridge in the axial direction.

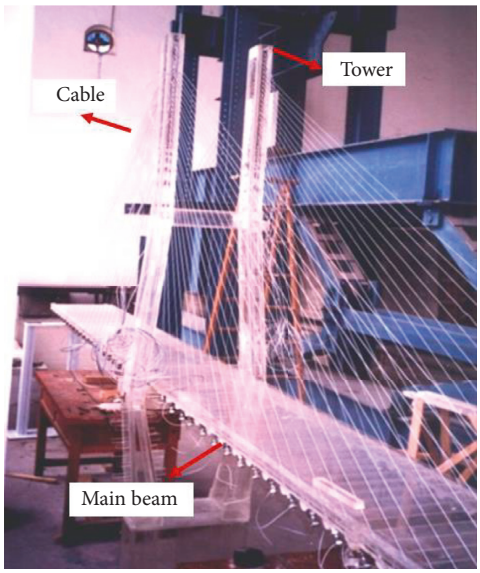

Figure 7: Experimental bridge model in hoisting stage.

prototype bridge, so the influence of material nonlinearity is no longer considered in the buckling analysis of the test bridge.

In this study, the space bar model of the fishbone beam model is used, and the stability analysis is performed by means of finite element software ANSYS. In the calculation model, the main beam, main tower, and main pier are all simulated by the beam element (*BEAM*4). Considering the tensile performance of the stayed cables, the rod unit (*LINK*10) is used to simulate, the end joints of the transverse member, and the force point of the stay cable on the main beam are connected by a rigid arm. For the stability analysis of cable-stayed bridges, the actual vehicle loads can be converted to a uniform load along the deck [18]. Since the main beam of the model is *BEAM*4 unit, the unit type can only work on the line distribution load. After calculation, the uniform load of the vehicle load is as follows: $q = 48.96N/\text{m}$.

Compared with the calculation conditions of the real bridge, only five construction stages and two conditions of the completed bridge state are selected in this analysis, and the linear stability analysis is carried out. The working conditions are as follows: No. 6 segments of construction completed; No. 14 segments of construction completed; No. 18 segments of construction completed; No. 23 segments of construction completed; side spans closed, and No. 27 segments of construction completed; completed bridge state under dead weight, and completed bridge state under the action of dead weight and full-bridge uniform load.

The eigenvalue method is used in ANSYS software, and the buckling safety factor and its corresponding instability mode of the experimental bridge under the above seven conditions are obtained. The results of linear stability analysis under various conditions are listed in Table 1. Through the stability analysis, the linear instability mode of

Table 1: Linear stability analysis situation of key stages.

Structure assembling state	Load cases	Constraint conditions	Linear instability λ of model test	Linear instability λ	Remarks
No. 6 segment	Dead weight, hanging basket	4# pier consolidation, tower and beam temporary consolidation	39.2	—	—
No. 14 segment			33.0		
No. 18 segment			28.4		
No. 23 segment			31.9	28.8	
No. 27 segment			18.1	—	Closure of side span
Finished bridge state	Dead weight	4# pier consolidation, 3# pier constraint	16.8		Closure of side span and midspan, cancel temporary constraints
Finished bridge state (full bridge uniform load)	Dead weight, vehicle load		15.3	12.4	

the experimental bridge under various conditions can be obtained. It can be seen from Table 1 that the linear stability safety factors of the bridge during the construction process and the finished bridge states are generally large. Comparing the linear instability λ values of the original bridge and the model bridge under the No. 23 segments and the uniform load state of the finished bridge, the linear instability λ value of the original bridge is slightly smaller than the model bridge. The reason is that: the influence of lateral wind load and cable pretension is considered in the calculation of the original bridge, but the analysis of the model bridge is not considered.

The instability modes of the original bridge and the model bridge are basically the same, and they are all in-plane instability failures.

Although the results of linear stability cannot actually describe the ultimate value of the bridge's buckling bearing capacity, its result can be used as the upper limit of nonlinear stability analysis, and it also represents the instability mode of the second kind of stability problem. The stress values calculated by linearity exceed the yield limit of the structure. However, the distribution of maximum stress can be roughly determined by analysis. For the tower, the maximum stress is distributed at the lower end of the upper column and the middle and lower columns; the maximum stress on the beam usually occurs near the position of the main tower.

Compared with the linear static analysis and linear buckling analysis of the original bridge and the model bridge under the No. 23 segments and the uniform load of the finished bridge, there is little difference between the two methods in instability modes and stress distribution. It can be preliminarily considered that the two methods are correct.

4.3. Model Test

4.3.1. Assembly and Test Procedures for the Model. According to the nonlinear stability analysis of the real bridge, the stability safety factor of the bridge during the completion phase of the construction of No. 23 segments and the operational phase of the bridge is small. Therefore, the model bridge will focus on the corresponding model test study on the stability of these two stages. The installation and testing procedures for the bridge model are as follows:

(1) Preparation, including the production of the main beam and tower pier and the production of anchoring devices of the model test.

(2) Installation of the main tower and pier

(3) The main beam is installed in segments, hanged, tensioned, and anchored cables, and the beams are temporarily fixed at the pier

(4) In the case of the largest double cantilever, cable tension adjustment is conducted and then the loading test is performed

(5) Close the side span, hoist the last segment, handle the symmetrical part, and cancel the temporary support

(6) The cable tension is adjusted according to the whole system, and the load test in the finished bridge state is carried out

A total of 154 strain observation points are arranged in the test. There are 20 control sections of the main beam with a total of 76 measuring points, 12 control sections of the main tower pier, and 1 control section of the lower cross beam with a total of 78 measuring points. It is known from the calculation that the stress of the middle and lower tower columns first reaches the maximum when the instability occurs, so the arrangement of the measuring points should be increased. There are 12 deformation observation points distributed in the vertical and horizontal directions of the tower top and the lower end of the upper tower. The deformation observation point is symmetrically arranged at the anchor position of the main beam 23# cable and 12# cable.

4.3.2. Static Load Experiment under the Maximum Cantilever. The stability problem of the cable-stayed bridge during the construction phase is very important and should be discussed. Therefore, the model test and analysis are only carried out for the maximum double cantilever construction stage of the original bridge. At the same time, it is necessary to take into account the subsequent tests. Therefore, its stability test does not require destruction, only to meet the minimum load conditions required by the specification [19]. According to the requirements of the current specification, its stability safety factor should reach 4.0. For this test, the maximum test load is taken to 400% times loading.

Table 2: Experimental conditions.

Experimental conditions	Load cases	Load configuration
The first load	100% times loading	The tower has a weight of 510 kg. The main beam is loaded with a total of 455 kg
The second load	Midspan + hanging basket	At the end of the midspan, a weight of 5.7 kg is used to simulate the hanging basket, when the main beam is asymmetrical
The third load	Midspan + hanging basket side span + hanging basket + closure segment	A 10.7 kg weight is added to the end of the side to simulate the hanging basket and the closing section
The fourth load	200% times loading	Remove the load applied for the second and third times and then load 500 kg symmetrically on the main beam
The fifth load	300% times loading	Load 500 kg symmetrically on the main beam
The sixth load	400% times loading	Load 500 kg symmetrically on the main beam

The whole test has a total of six times loadings. The loading method is to symmetrically and uniformly lay the concrete blocks or bricks in the range of 2×20 cm on the main girder bridge deck, to make it as close as possible to uniform loading. Each loading situation is seen in Table 2. The following data need to be measured throughout the test: beam and tower strain and deformation. The value is a relative increment. After each loading, the cable forces are measured, but the measured values are absolute values. After the main tower weight is completed, the main beam is not yet weighted.

4.4. Test Results. The measured values of cable forces under 100%, 200%, 300%, and 400% times loading are compared with each other, as shown in Figure 8. It can be seen from the figure that the increase of cable force is uniform under each loading condition. According to the tensile test of the wire rope used for the model, the breaking force is about 2000 N. When the maximum load is 400% times, the cable force is less than 450 N, so it can be said that the wire rope fully meets the strength requirements.

The stress test values and relative comparison relations of the main beams under 200%, 300%, and 400% times loading are measured in the test , as shown in Figure 9. It can be seen that the stress increments of the main beam at the 4-4, 5-5, and 9-9 sections are not uniform, and the stresses of the 6-6 and 9-9 sections are the largest under each load condition. The stress test values and relative comparison relations of the towers under 200%, 300%, and 400% times loading are measured, as shown in Figure 10. It can be seen from Figure 10 that under various load conditions, the stress increments at the lower end of the upper tower column, the upper end of the middle tower column, the lower end of the middle tower column, and the lower end of the lower tower column are larger. The change of stress increment is more uniform. The displacement changes of the main beam and tower under 200%, 300%, and 400% times loading and their relative comparative relations can be obtained from the test results, as shown in Figure 11. It can be seen from Figure 11 that, under 400% times loading, the maximum vertical deflection of the beam is 21.32 mm, which is 127.92 cm in the real bridge. However, the relative displacement of the beam and the tower changes uniformly during the loading process. Considering the material influence of the plexiglass itself, the deformation is larger. It can be considered that the structure still satisfies the carrying capacity at this stage, but the deformation is too large, which is close to the state of instability.

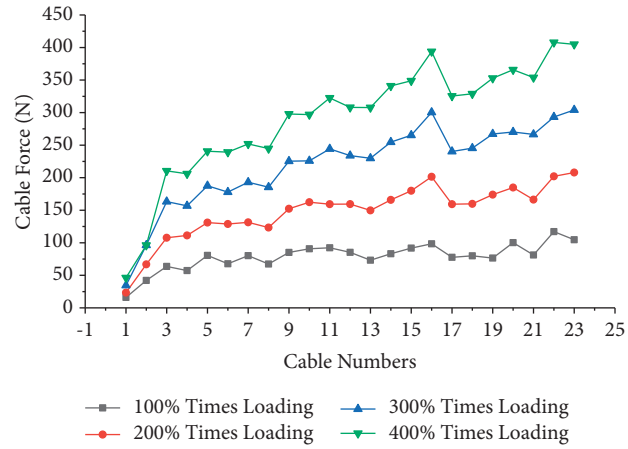

Figure 8: Comparisons of cable forces under 100%~400% times loading.

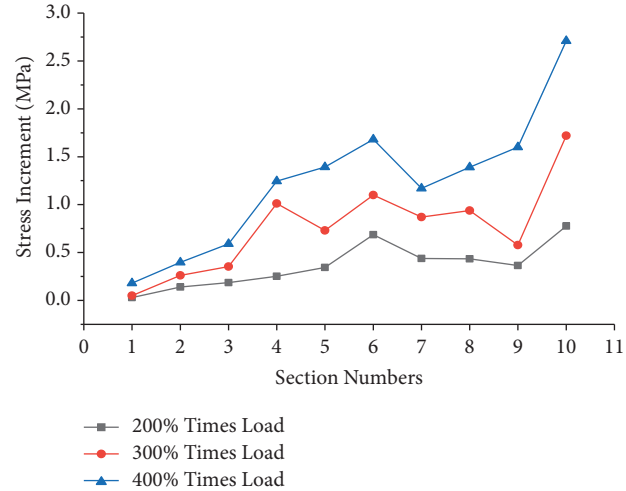

Figure 9: Stress variation of the main beam under 200%~400% times loading.

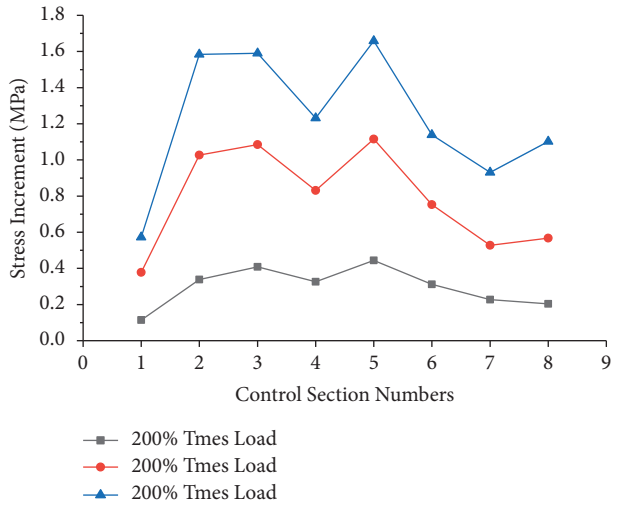

Figure 10: Stress changes in the main tower under 200%~400% times loading.

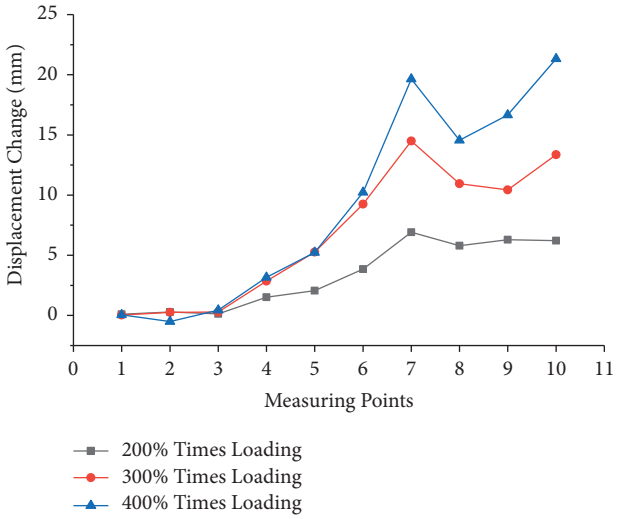

Figure 11: Variation of displacement of main beam and tower under 200%~400% times loading.

According to the theoretical calculation, the deformation of the symmetrical structure under the action of the symmetrical load should also be symmetrical. For the difference in test results, in addition to the production error, the symmetric loading of the load is also a key problem. In the process of the field test, it is found that the order of loading is also important. When the midspan loading is advanced, stop the midspan loading and wait for the side span to be applied to the same size load, the displacement meter reading is still difficult to balance, and the midspan displacement reading is greater than the displacement reading at the same symmetrical position of the side span. The reason for this phenomenon is that when the eccentric load is applied, the tower column is inclined and deformed toward the side, and after applying a counterbalance force in the opposite direction, the deformation of the column of the plexiglass material requires a slow recovery process. This phenomenon can also happen for concrete materials. To better ensure the symmetry of the structure stress and deformation, the methods of loading, observing, and adjusting the loading sequence are taken into account when loading, and the test results are satisfactory.

5. Conclusion

(1) Through the model test, the bearing capacity and deformation of the structure under various conditions can be known. For example, under the action of an unbalanced load, the stress and deformation of the structure have practical significance for the unbalanced construction during the construction process.

(2) The correctness of the calculation method is checked by comparing the measured results of the model test with the theoretical calculation. In addition, the measured results of the model are extended to the original bridge according to the similarity relationship, which provides a reference for the design and construction of the real bridge. The test results of the bridge show that the structure can still withstand 400% times loading under the maximum single cantil every state; that is to say, the stability safety factor of the bridge at this stage meets the requirement of safety factor value 4.0 stipulated in the code.

(3) According to the calculation and analysis of a PC cable-stayed bridge, the second kind of stability safety factor after considering nonlinearity is less than the safety factor of linear instability. Therefore, the second kind of stable safety factor should be used as the basis for discriminating structural instability.

(4) According to the similarity relationship, the model of the bridge is fabricated, and the model test and analysis of the largest single cantilever state are carried out. The model of the bridge is still substantially in the elastic range under 400% times loading. It is concluded that the bridge meets the stability requirements during the construction phases.

(5) Since the plexiglass material used in the model bridge does not fully simulate the material properties of the concrete of the real bridge, the nonlinearity of the material is not well simulated in this model test. In addition, the effects of concrete shrinkage, creep, and prestressing effects on the stability of cable-stayed bridges are not discussed in this paper. Through the analysis of the force and deformation under various conditions at this stage, the working state of the model is in the elastic range, and the influence of material nonlinearity is difficult to simulate in this model test. Whether the stability of the bridge meets the requirements in the completed bridge state and operation stage needs further testing and verification.

Data Availability

All data generated or analyzed during this study are included in this article and are available upon request by contact with the corresponding author.

Disclosure

The content of the paper belongs to the authors' personal point of view and does not represent the position of the funding.

Conflicts of Interest

The authors declare that they have no conflicts of interest.

Acknowledgments

The support of the Natural Science Foundation of China (Grant No. 51908093), Chongqing Returned Overseas Scholars' Entrepreneurship and Innovation Support Fund (cx2018113 and cx2020117), and National Key Laboratory of Mountain Bridge and Tunnel Engineering Development Fund (CQSLBF−Y14 and CQSLBF−Y16−10) are greatly appreciated.

References

[1] Y. Bu, L. Zhao, and Q. Zhang, "Structural nonlinear stability analysis of Sutong Yangtze river bridge," *China Civil Engineering Journal*, vol. 46, no. 01, pp. 84–91, 2013.

[2] G. Li, *Stability and Vibration of Bridge structures*, China, Railway Publishing House, Beijing, 1992 (in Chinese).

[3] Y. Zeng, Yu Qu, and Q. Zhou, "Analysis of fatigue cracking of orthotropic steel decks using XFEM," *Engineering Failure Analysis*, vol. 140, 2022.

[4] H.-S. Shu and Y.-C. Wang, "Stability analysis of box-girder cable-stayed bridges," *Journal of Bridge Engineering*, vol. 6, no. 1, pp. 63–68, 2001.

[5] X. Yang, *Research on the Nonlinear Behavior of Long-Span cable-stayed Bridges Considering Overall Construction process*, Southwest Jiaotong University, Chengdu, 2007, (in Chinese).

[6] J. Cheng, L. Xiao, and H. Xiang, "Full range nonlinear aerostatics analysis for long-span cable-stayed bridge," *China Journal of Highway and Transport*, no. 03, pp. 27–30, 2000.

[7] L. Zhao and X. Yang, "Stablity analysis of the second nanjing yangtze river cable—stayed bridge during construction," *Journal of Highway and Transportation Research and Development*, vol. 22, no. 7, pp. 78–81, 2005, (in Chinese).

[8] M. Yangjun, L. Can, Y. Meng, and C Li, "Analysis of wind-resistant and stability for cable tower in cable-stayed bridge with four towers," *IOP Conference Series: Earth and Environmental Science*, vol. 69, no. 1, Article ID 012192, 2017.

[9] X. Deng and M. Liu, "Nonlinear Stability Analysis of a Composite Girder Cable-Stayed Bridge with Three Pylons during Construction," *Mathematical Problems in Engineering*, vol. 2015, Article ID 978514, 9 pages, 2015.

[10] X. Nagaim, "Static and dynamic instability analysis of 1400-meter long-span cable-stayed bridges," *IABSE Symposium Kobe 1998, IABSE Reports*, vol. 79, pp. 281–286, 1998.

[11] J. Z. Xin, Y. Jiang, J. T. Zhou, L. Peng, S. Liu, and Q Tang, "Bridge deformation prediction based on SHM data using improved VMD and conditional KDE," *Engineering Structures*, vol. 261, Article ID 114285, 2022.

[12] J. Zhong, M. Ni, H. Hu, W. Yuan, H. Yuan, and Y. Pang, "Uncoupled multivariate power models for estimating performance-based seismic damage states of column curvature ductility," *Structures*, vol. 36, pp. 752–764, 2022.

[13] JTG/TD 65-01-2007, *Guidelines for Design of Highway cable-stayed bridge*, China Communication Press, Beijing, 2007, (in Chinese).

[14] Li Na Yue and S. Li, "The finite element model updating of long span cable-stayed bridge based on static and dynamic loading test," *Applied Mechanics and Materials*, vol. 3468, no. 644, 2014.

[15] Q. Z. Tang, J. Z. Xin, Y. Jiang, J. Zhou, S. Li, and L. Fu, "Fast identification of random loads using the transmissibility of power spectral density and improved adaptive multiplicative regularization," *Journal of Sound and Vibration*, vol. 534, Article ID 117033, 2022.

[16] Z. Yang, M. Sun, Y. Liu, Y. Qu, Y. Zhang, and X. Xie, "Stability analysis of synchronous construction of towers and beams of cable-stayed bridge," *IOP Conference Series: Materials Science and Engineering*, vol. 397, no. 1, Article ID 012011, 2018.

[17] T. Wusheng, L. Bin, and J. Xingliang, "Study on static and dynamic characteristics analysis of long span steel concrete composite beam cable-stayed bridge," in *Proceedings of the 2017 6th International Conference on Energy, Environment and Sustainable Development (ICEESD 2017)*, Jiangsu, China, January, 2017.

[18] Q. Z. Tang, J. Z. Xin, Y. Jiang, J. Zhou, S. Li, and Z. Chen, "Novel identification technique of moving loads using the random response power spectral density and deep transfer learning," *Measurement*, vol. 195, no. 12, Article ID 111120, 2022.

[19] B. Alemdar, T. Temel, T. Janusz, K. Altok, and E. Arif, "Static and dynamic field load testing of the long span Nissibi cable-stayed bridge," *Soil Dynamics and Earthquake Engineering*, vol. 94, 2017.